

Magnons and excitation continuum in XXZ triangular antiferromagnetic model: Application to Ba₃CoSb₂O₉

E. A. Ghioldi,¹ A. Mezio,¹ L. O. Manuel,¹ R. R. P. Singh,² J. Oitmaa,³ and A. E. Trumper¹¹*Instituto de Física Rosario (CONICET) and Universidad Nacional de Rosario, Boulevard 27 de Febrero 210 bis, (2000) Rosario, Argentina*²*Department of Physics, University of California, Davis, California 95616, USA*³*School of Physics, The University of New South Wales, Sydney 2052, Australia*

(Received 14 November 2014; revised manuscript received 20 February 2015; published 22 April 2015)

We investigate the excitation spectrum of the triangular-lattice antiferromagnetic XXZ model using series expansion and mean field Schwinger boson approaches. The single-magnon spectrum computed with series expansion exhibits rotonic minima at the middle points of the edges of the Brillouin zone, for all values of the anisotropy parameter in the range $0 \leq J^z/J \leq 1$. Based on the good agreement with series expansion for the single-magnon spectrum, we compute the full dynamical magnetic structure factor within the mean field Schwinger boson approach to investigate the relevance of the XXZ model for the description of the unusual spectrum found recently in Ba₃CoSb₂O₉. In particular, we obtain an extended continuum above the spin wave excitations, which is further enhanced and brought closer to those observed in Ba₃CoSb₂O₉ with the addition of a second neighbor exchange interaction approximately 15% of the nearest-neighbor value. Our results support the idea that excitation continuum with substantial spectral-weight are generically present in two-dimensional frustrated spin systems and fractionalization in terms of *bosonic* spinons presents an efficient way to describe them.

DOI: [10.1103/PhysRevB.91.134423](https://doi.org/10.1103/PhysRevB.91.134423)

PACS number(s): 75.10.Jm, 75.40.Gb

I. INTRODUCTION

The study of two dimensional (2D) quantum spin liquids (QSL) has been one of the central topics in condensed matter physics. Aided by frustration and strong quantum fluctuations, novel quantum spin-liquid phases can emerge in quantum spin systems, which do not break any symmetry of the Hamiltonian and there is no local order parameter to unambiguously characterize them. Consequently, conventional paradigms of magnetism such as spin waves or Landau-Ginzburg-Wilson theories turn out to be inadequate [1–6]. Several candidate materials showing such spin liquid behavior have been indirectly identified by specific heat or nuclear relaxation measurements [7], however, a direct experimental detection of QSL remains elusive.

Another signature of QSL is the emergence of spin- $\frac{1}{2}$ fractional excitations, called spinons. They have been predicted [8] in 1D AF's and detected [9] by means of inelastic neutron scattering (INS) experiments. Here, the spinon excitation is interpreted as a propagating domain wall; while the observed extended continuum in the spectrum is related to the different pairs of independently propagating spinons created in the AF system once spin-1 excitations are exchanged with the scattering of neutrons.

In 2D the physical origin of spinons and their quantum statistics is more complex and not fully understood. However, it is widely believed that the extended continuum observed with INS in certain 2D compounds may also correspond to the fractionalization phenomenon. Such a continuum has been observed in the inorganic compound [10] Cs₂CuCl₄, the kagome-lattice Herbertsmithites ZnCu(OH)Cl [11] and, recently [12], in Ba₃CoSb₂O₉ which is an experimental realization of the spin- $\frac{1}{2}$ triangular antiferromagnet, with very little spatial distortion [13]. In Cs₂CuCl₄ the superexchange interactions are spatially anisotropic [10], while in Ba₃CoSb₂O₉ there is enough evidence of anisotropic spin spin interactions

described by the XXZ model in the easy-plane regime but little deviation from the triangular-lattice geometry [14,15]. While the Herbertsmithite materials remain disordered down to the lowest measured temperature, at sufficiently low temperatures, Cs₂CuCl₄ and Ba₃CoSb₂O₉ are magnetically ordered, showing helical [10] and 120° long range Néel order [12], respectively. In the case of Cs₂CuCl₄ the spectrum shows well defined magnon signals at the Goldstone modes and a broad continuum with a dominant spectral weight at higher energies that persist even above the Néel temperature $T_N = 0.62$ K. Due to the 2D character of the magnetic interactions this behavior was originally associated with the experimental realization of 2D spinons [10], however, further theoretical work showed that spinons in Cs₂CuCl₄ are actually of 1D character [16], that is, the combined effect of spatially anisotropic quantum fluctuations and frustration induce an unexpected dimensional reduction [5,17,18]. In contrast, though anisotropic in spin space, the magnetic interactions in Ba₃CoSb₂O₉ are 2D spatially isotropic. Therefore, the unusual broad and dominant continuum above the spin wave dispersion recently found below $T_N = 3.8$ K has been interpreted as a true 2D fractionalization, suggesting that the 120° Néel phase of this compound may be in close proximity to a spin liquid phase [12,19].

In this article we investigate the energy spectrum of the triangular AF XXZ model using two complementary techniques, series expansion (SE) and mean field Schwinger bosons (SBMF) [20–24]. Series expansion gives reliable results for the dispersion relation of the single-magnon sector of the spectrum while a Schwinger bosons mean field allows us to study the whole energy spectrum with a spinon based theory through the dynamical magnetic structure factor [20]. In order to take into account anisotropic exchange interactions within the SBMF approximation we have used four bond operators, as proposed by Burkov and Mac Donald within the context

of quantum Hall bilayers [25]. Our series expansion results show the presence of rotonlike minima at the middle of the edges of the Brillouin zone that persist down to the XY model. Motivated by the good agreement between series expansion and SBMF theory for the one magnon dispersion relation and based on the probable proximity of $\text{Ba}_3\text{CoSb}_2\text{O}_9$ to a spin liquid phase we study the effect of second neighbor exchange interactions on the whole spectrum of the XXZ model using SBMF theory. In particular, we find that a 15% second neighbor interaction is enough to reproduce an extended continuum above the magnon excitations. For this frustration value there is a weakening of the attractive interaction between the two spinons building up the magnon excitation along with a strong reduction of the local magnetization. Therefore, our study provides a consistent calculation supporting the recently proposed idea of fractionalization of 2D magnon excitations in $\text{Ba}_3\text{CoSb}_2\text{O}_9$ [12].

The antiferromagnetic XXZ model is defined as

$$H = \sum_{\langle ij \rangle} [J(S_i^x S_j^x + S_i^y S_j^y) + J^z S_i^z S_j^z], \quad (1)$$

where the sum is over the nearest neighbor sites $\langle ij \rangle$ of a triangular lattice. This Hamiltonian breaks the $SU(2)$ symmetry of the Heisenberg model down to a $U(1) \times Z_2$. In the easy plane case $0 \leq J^z/J \leq 1$ and in the thermodynamic limit the $U(1)$ symmetry is broken by the ground state, selecting a 120° Néel order state lying in the $x - y$ plane. This seems to be the case for the compound $\text{Ba}_3\text{CoSb}_2\text{O}_9$ below $T_N = 3.8$ K.

II. SERIES EXPANSION CALCULATION

To develop the series expansion, we first rewrite the Hamiltonian in a rotated basis, where the z axis points along the local spin direction of the 120° ordered phase [26–28]. Then the Hamiltonian is written as $H_0 + \lambda V$, where H_0 consists of only Ising terms, with simple eigenstates and a ground state that corresponds to one of the classical ground states. All other terms of the Hamiltonian are placed in V . The parameter λ is introduced artificially as an expansion parameter. The Hamiltonian of interest is realized at $\lambda = 1$. An additional ordering field term with coefficient $t(1 - \lambda)$, with arbitrary t is used to improve the convergence of the series [27]. Series expansion for the ground state energy and the order parameter for the 120° Néel order were developed for various values of the anisotropy $\alpha = J^z/J$ complete to order λ^{11} . To analyze the magnetization series, we perform a change of variables to remove a square-root singularity at $\lambda = 1$ [27,28] and then develop d-log Padé approximants. The estimated magnetization are shown in Table I where the reduction of the zero point quantum fluctuations is clearly observed as anisotropy is increased.

The one-particle effective Hamiltonian is calculated as a power series in λ for various real-space distances from which the spectra at any wave vector are readily obtained by Fourier transformation. These spectra are extrapolated to $\lambda = 1$ by Padé approximants. Calculations were done to order λ^8 . We checked that the series for the Heisenberg model ($J^z = J$) agreed completely with those obtained before [26]. The SE results are shown in Fig. 1 (magenta dots) where

TABLE I. Local magnetization m of the 120° Néel ground state of the spin- $\frac{1}{2}$ antiferromagnetic XXZ model on the triangular lattice obtained within the present mean field Schwinger bosons (SBMF), the linear spin wave theory (LSWT), and series expansion.

J^z/J	SBMF	LSWT	Series
1	0.2739	0.2386	0.198 ± 0.034
0.8	0.3402	0.3522	0.245 ± 0.026
0.6	0.3663	0.3858	0.283 ± 0.023
0.4	0.3862	0.4096	0.314 ± 0.018
0.0	0.4204	0.4485	0.403 ± 0.005

the predicted single-magnon spectrum shows the expected Goldstone mode structure at $\mathbf{k} = (0,0), \pm(\frac{4\pi}{3},0)$ (points O, Q, and C of Fig. 1) for the isotropic case ($J^z = J$) and at $\mathbf{k} = (0,0)$ for the anisotropic case ($J^z < J$). Furthermore, the SE results exhibit rotonlike minima at the middle points of the edges of the Brillouin zone (point B of Fig. 1). Though not shown in the figure we found that the rotonic excitation persists down to the XY model case ($J^z/J = 0$) [29]. These excitation should not be identified to the local minima at momentum $\mathbf{k} = \pm(\frac{4\pi}{3},0)$ whose appearance is due to anisotropy effects. Originally, for the isotropic Heisenberg case, the rotonic excitations were described in terms of pairs of spinons [18] or vortex-antivortex [30] excitations with fermionic character, or with conventional multimagnon excitations in noncollinear antiferromagnets [29,31]. Alternatively, it was shown that the high entropy values found with high temperature expansion [32] could be reconciled by assuming a bosonic character for the rotonic excitations [26] which within the Schwinger boson language can be interpreted as a pair of weakly bound spinon excitations [33] (see below).

III. SCHWINGER BOSONS FOR THE XXZ MODEL

In this section, we further extend the widely used Schwinger boson representation to the XXZ model. In contrast to the isotropic case [20,23] and previous extensions [34,35] of the anisotropic case, we express the spin spin interaction in terms of four bond operators, as proposed by Burkov and MacDonald [25], in order to preserve the original $U(1) \times Z_2$ symmetry of the Hamiltonian. Then, the magnetically 120° Néel order state that breaks the $U(1)$ symmetry is manifested by a Schwinger boson condensation which naturally occurs in the theory without assuming it from the beginning [21,22].

Within the Schwinger bosons representation the spin operator components are written in terms of spin- $\frac{1}{2}$ bosons b_\uparrow and b_\downarrow as

$$\hat{S}_i^x = \frac{1}{2}(\hat{b}_{i\uparrow}^\dagger \hat{b}_{i\downarrow} + \hat{b}_{i\downarrow}^\dagger \hat{b}_{i\uparrow}), \quad \hat{S}_i^y = \frac{1}{2i}(\hat{b}_{i\uparrow}^\dagger \hat{b}_{i\downarrow} - \hat{b}_{i\downarrow}^\dagger \hat{b}_{i\uparrow}), \quad (2)$$

$$\hat{S}_i^z = \frac{1}{2}(\hat{b}_{i\uparrow}^\dagger \hat{b}_{i\uparrow} - \hat{b}_{i\downarrow}^\dagger \hat{b}_{i\downarrow}), \quad (3)$$

where the local constraint

$$\sum_{\sigma} \hat{b}_{i\sigma}^\dagger \hat{b}_{i\sigma} = 2s \quad (4)$$

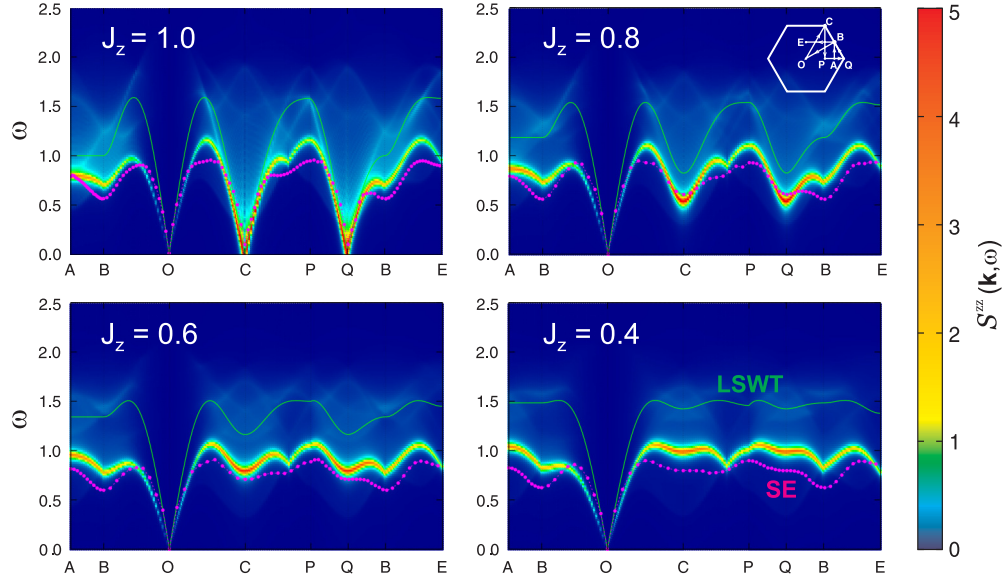


FIG. 1. (Color online) Relation dispersion predicted by series expansion (magenta dots) and dynamical structure factor computed within the reconstructed SBMF theory (intensity curves), along the path of the Brillouin zone shown in the inset, for several anisotropy values. The LSWT results (thin green line) are shown for comparison. Inset: path of the Brillouin zone, $O = (0,0)$, $P = (\frac{2\pi}{3}, 0)$, $A = (\pi, 0)$, $B = (\pi, \frac{\pi}{\sqrt{3}})$, $C = (\frac{2\pi}{3}, \frac{\pi}{\sqrt{3}})$, $Q = (\frac{4\pi}{3}, 0)$, and $E = (0, \frac{\pi}{\sqrt{3}})$. The values of J_z are in units of J .

must be imposed to fulfill the spin algebra. The relevant bond operators for the XXZ Hamiltonian Eq. (1) are

$$\hat{A}_{ij} = \frac{1}{2}(b_{i\uparrow}b_{i\downarrow} - b_{i\downarrow}b_{j\uparrow}), \quad \hat{B}_{ij} = \frac{1}{2}(b_{i\uparrow}b_{j\uparrow} + b_{i\downarrow}b_{j\downarrow}), \quad (5)$$

$$\hat{C}_{ij} = \frac{1}{2}(b_{i\uparrow}b_{j\uparrow}^\dagger - b_{i\downarrow}b_{j\downarrow}^\dagger), \quad \hat{D}_{ij} = \frac{1}{2}(b_{i\uparrow}b_{j\downarrow} + b_{i\downarrow}b_{j\uparrow}), \quad (6)$$

where \hat{A}_{ij} and \hat{B}_{ij} are $SU(2)$ and time reversal invariant, while \hat{C}_{ij} and \hat{D}_{ij} are $U(1)$ invariant (rotation around z axis) and change sign, $\hat{C}_{ij} \rightarrow -\hat{C}_{ij}$, $\hat{D}_{ij} \rightarrow -\hat{D}_{ij}$, under time reversal [36]. Then, after writing down the spin operators in terms of Schwinger bosons, Eq. (1) results in

$$H = \frac{1}{2} \sum_{\langle ij \rangle} [(J + J^z)(\hat{B}_{ij}^\dagger \hat{B}_{ij} : -\hat{A}_{ij}^\dagger \hat{A}_{ij}) - (J - J^z)(\hat{C}_{ij}^\dagger \hat{C}_{ij} : -\hat{D}_{ij}^\dagger \hat{D}_{ij})]. \quad (7)$$

Noticing that the inversion of S_i^z can be carried on as a time reversal operation followed by a π angle rotation around z axis, it is easy to check that the original $U(1) \times Z_2$ symmetry of the XXZ model is preserved by Eq. (7).

A. Mean field approximation

Now a nontrivial mean field decoupling of Eqs. (7) can be implemented as

$$\hat{X}_{ij}^\dagger \hat{X}_{ij} \approx \langle \hat{X}_{ij}^\dagger \rangle \hat{X}_{ij} + \hat{X}_{ij}^\dagger \langle \hat{X}_{ij} \rangle - \langle \hat{X}_{ij}^\dagger \rangle \langle \hat{X}_{ij} \rangle, \quad (8)$$

where $\hat{X} = \hat{A}, \hat{B}, \hat{C}$, and \hat{D} . From all the possible *Ansätze* we choose translational invariant mean field parameters such as $\langle \hat{A}_{ij} \rangle = \iota A_{ij}$, $\langle \hat{C}_{ij} \rangle = \iota C_{ij}$, $\langle \hat{B}_{ij} \rangle = B_{ij}$, and $\langle \hat{D}_{ij} \rangle = D_{ij}$ with $A_{ij} = -A_{ji}$, $C_{ij} = -C_{ji}$, $B_{ij} = B_{ji}$, and $D_{ij} = D_{ji}$ all real. In principle, the resulting mean field Hamiltonian H_{MF} breaks the time reversal symmetry which followed by

the π angle rotation around z realizes the S_i^z inversion. So, the Z_2 symmetry seems to be broken. However, if H_{MF} is gauge transformed as $G_T^{-1} H_{MF} G_T = H'_{MF}$, where $G_T : b_\sigma \rightarrow b_\sigma e^{-i\frac{\pi}{4}}$, time reversal symmetry is restored by H'_{MF} and consequently the Z_2 symmetry is also preserved. Actually we choose the above *Ansatz* because in the thermodynamic limit it is compatible with the semiclassical 120° Néel state lying in the $x-y$ plane [37]. Replacing Eq. (8) in Eq. (7) and following the standard procedure [38] we arrive at the diagonalized mean field Hamiltonian

$$\hat{H}_{MF} = \sum_{\mathbf{k}} \omega_{\mathbf{k}\uparrow} \alpha_{\mathbf{k}\uparrow}^\dagger \alpha_{\mathbf{k}\uparrow} + \omega_{-\mathbf{k}\downarrow} \alpha_{-\mathbf{k}\downarrow}^\dagger \alpha_{-\mathbf{k}\downarrow} + E_{MF}, \quad (9)$$

with the spinon relation dispersion defined as

$$\omega_{\mathbf{k}\uparrow} = \omega_{-\mathbf{k}\downarrow} = \omega_{\mathbf{k}} = \sqrt{[\Gamma_{\mathbf{k}}^{BC} + \lambda]^2 - [\Gamma_{\mathbf{k}}^{AD}]^2}, \quad (10)$$

with

$$\Gamma_{\mathbf{k}}^{BC} = \frac{1}{2} \left(1 + \frac{J^z}{J} \right) \gamma_{\mathbf{k}}^B - \frac{1}{2} \left(1 - \frac{J^z}{J} \right) \gamma_{\mathbf{k}}^C,$$

$$\Gamma_{\mathbf{k}}^{AD} = \frac{1}{2} \left(1 + \frac{J^z}{J} \right) \gamma_{\mathbf{k}}^A - \frac{1}{2} \left(1 - \frac{J^z}{J} \right) \gamma_{\mathbf{k}}^D,$$

and

$$\gamma_{\mathbf{k}}^A = \sum_{\delta>0} J A_\delta \sin(\mathbf{k} \cdot \delta), \quad \gamma_{\mathbf{k}}^B = \sum_{\delta>0} J B_\delta \cos(\mathbf{k} \cdot \delta),$$

$$\gamma_{\mathbf{k}}^C = \sum_{\delta>0} J C_\delta \sin(\mathbf{k} \cdot \delta), \quad \gamma_{\mathbf{k}}^D = \sum_{\delta>0} J D_\delta \cos(\mathbf{k} \cdot \delta),$$

where $\delta = \mathbf{r}_j - \mathbf{r}_i$ are the vectors connecting the first neighbors of the triangular lattice. The ground state mean field

energy results in

$$\begin{aligned} E_{\text{MF}} &= \frac{1}{2} \sum_{\mathbf{k}} \omega_{\mathbf{k}} - \lambda(2S + 1)N \\ &= 3N[(J + J^z)(B_{\delta}^2 - A_{\delta}^2) - (J - J^z)(C_{\delta}^2 - D_{\delta}^2)]. \end{aligned} \quad (11)$$

Notice that λ is the Lagrange multiplier introduced to enforce, on average, the local constraint of Eq. (4).

The self consistent mean field equations are

$$S + \frac{1}{2} = \frac{1}{2N} \sum_{\mathbf{k}} \frac{\Gamma_{\mathbf{k}}^{\text{BC}} + \lambda}{\omega_{\mathbf{k}}}, \quad (12)$$

$$A_{\delta} = \frac{1}{2N} \sum_{\mathbf{k}} \frac{\Gamma_{\mathbf{k}}^{\text{AD}}}{\omega_{\mathbf{k}}} \sin(\mathbf{k} \cdot \delta), \quad (13)$$

$$B_{\delta} = \frac{1}{2N} \sum_{\mathbf{k}} \frac{\Gamma_{\mathbf{k}}^{\text{BC}} + \lambda}{\omega_{\mathbf{k}}} \cos(\mathbf{k} \cdot \delta), \quad (14)$$

$$C_{\delta} = \frac{1}{2N} \sum_{\mathbf{k}} \frac{\Gamma_{\mathbf{k}}^{\text{BC}} + \lambda}{\omega_{\mathbf{k}}} \sin(\mathbf{k} \cdot \delta), \quad (15)$$

$$D_{\delta} = \frac{1}{2N} \sum_{\mathbf{k}} \frac{\Gamma_{\mathbf{k}}^{\text{AD}}}{\omega_{\mathbf{k}}} \cos(\mathbf{k} \cdot \delta). \quad (16)$$

As we have pointed out the present mean field approximation preserves the original $U(1) \times Z_2$ symmetry of the XXZ Hamiltonian. Nonetheless, it turns out that the minimum of the spinon dispersion at $\frac{\mathbf{Q}}{2}$ behaves as $\omega_{\frac{\mathbf{Q}}{2}} \rightarrow 1/N$, implying the occurrence of a Bose condensation of \hat{b}_{\uparrow} and \hat{b}_{\downarrow} at $\mathbf{k} = \frac{\mathbf{Q}}{2}$ and $\mathbf{k} = -\frac{\mathbf{Q}}{2}$, respectively, in the thermodynamic limit [see Eq. (10)]. This is interpreted as the rupture of the continuous $U(1)$ symmetry. In particular, by working out the static structure factor the singular mode, $\mathbf{k} = \frac{\mathbf{Q}}{2}$, of Eqs. (12)–(16) can be simply related to the local magnetization m and, after converting the sums into integrals, a new set of self consistent equations is obtained corresponding to the thermodynamic limit [21,22,39]. Alternatively, there is another way to compute the local magnetization m that we have checked to be completely equivalent to the previous one, which consists of solving the self consistent Eqs. (12)–(16) for finite size systems and then perform a size scaling of the expression [38],

$$m = \frac{1}{2N} \frac{\Gamma_{\frac{\mathbf{Q}}{2}}^{\text{BC}} + \lambda}{\omega_{\frac{\mathbf{Q}}{2}}}, \quad (17)$$

which in the thermodynamic limit corresponds to the singular mode of Eq. (12) when $\mathbf{Q} = (\frac{4\pi}{3}, 0)$ is the magnetic wave vector of the 120° Néel order. In Table I is shown the local magnetization m predicted by the SBMF for several anisotropy values resulting from the extrapolation of Eq. (17) in the thermodynamic limit. The predictions of series expansion and linear spin wave theory are also shown for comparison. It is worth stressing that the SBMF predictions compare quite well with that of series expansion as soon as anisotropy is increased.

B. Dynamical structure factor

In this subsection we study the spectrum by computing the zz component of the spin spin dynamical structure factor, $S^{zz}(\mathbf{k}, \omega) = \frac{1}{2\pi} \int_{-\infty}^{\infty} \langle S_{\mathbf{k}}^z(t) S_{-\mathbf{k}}^z(0) \rangle \exp^{i\omega t} dt$. The computation and the interpretation of the spectrum is based on our previous work performed for the isotropic case [38]. Here we also work on finite systems so the continuous $U(1)$ symmetry is, in principle, preserved. However, one can access the thermodynamic limit by extrapolating from finite size systems, as we previously did for the local magnetization study (Sec. III A). In fact, as soon as the long range 120° Néel order is developed in the $x - y$ plane the spectrum corresponding to the transversal spin-1 excitations can be obtained. Even if the calculation is similar to the isotropic case we consider it appropriate to outline again the main steps in order to develop a self contained subsection and to point out the differences that turn out for the XXZ case. Following Refs. [38,40,41] the dynamical structure factor within the mean field Schwinger bosons results in

$$\begin{aligned} S^{zz}(\mathbf{k}, \omega) &= \frac{1}{4N} \sum_{\mathbf{q}} (u_{\mathbf{q}} v_{\mathbf{k}+\mathbf{q}} - u_{\mathbf{k}+\mathbf{q}} v_{\mathbf{q}})^2 \\ &\quad \times \delta(\omega - (\omega_{\mathbf{q}\uparrow} + \omega_{\mathbf{k}-\mathbf{q}\downarrow})), \end{aligned} \quad (18)$$

where $u_{\mathbf{k}} = [\frac{1}{2}(1 + \frac{\Gamma_{\mathbf{k}}^{\text{BC}} + \lambda}{\omega_{\mathbf{k}}})]^{\frac{1}{2}}$ and $v_{\mathbf{k}} = \text{sgn}(\Gamma_{\mathbf{k}}^{\text{AD}}) [\frac{1}{2}(-1 + \frac{\Gamma_{\mathbf{k}}^{\text{BC}} + \lambda}{\omega_{\mathbf{k}}})]^{\frac{1}{2}}$ are the coefficients of the Bogoliubov transformation that diagonalizes \hat{H}_{MF} . $S^{zz}(\mathbf{k}, \omega)$ consists of two free spinon excitations that give rise to a continuum. However, two distinct contributions can be identified in the spectrum,

$$S^{zz}(\mathbf{k}, \omega) = S_{\text{sing}}^{zz}(\mathbf{k}, \omega) + S_{\text{cont}}^{zz}(\mathbf{k}, \omega), \quad (19)$$

where the singular part $S_{\text{sing}}^{zz}(\mathbf{k}, \omega)$ represents the process of destroying one spinon $b_{-\frac{\mathbf{Q}}{2}\downarrow}$ ($b_{\frac{\mathbf{Q}}{2}\uparrow}$) of the condensate and creating another one $b_{\frac{\mathbf{Q}}{2}\uparrow}^{\dagger}$ ($b_{-\frac{\mathbf{Q}}{2}\downarrow}^{\dagger}$) in the normal fluid, while the continuum part $S_{\text{cont}}^{zz}(\mathbf{k}, \omega)$ corresponds to the process of creating two spinons in the normal fluid only. Using the fact that $u_{\frac{\mathbf{Q}}{2}} = v_{\frac{\mathbf{Q}}{2}} \sim (Nm)^{\frac{1}{2}}$ and $\omega_{\frac{\mathbf{Q}}{2}\uparrow} = \omega_{\frac{\mathbf{Q}}{2}\downarrow} \sim 0$, the singular part can be approximated as

$$\begin{aligned} S_{\text{sing}}^{zz}(\mathbf{k}, \omega) &\approx \frac{m}{4} (v_{\mathbf{k}+\frac{\mathbf{Q}}{2}} - u_{\mathbf{k}+\frac{\mathbf{Q}}{2}})^2 \delta(\omega - \omega_{\mathbf{k}+\frac{\mathbf{Q}}{2}\uparrow}) \\ &\quad + \frac{m}{4} (u_{\frac{\mathbf{Q}}{2}-\mathbf{k}} - v_{\frac{\mathbf{Q}}{2}-\mathbf{k}})^2 \delta(\omega - \omega_{\mathbf{k}-\frac{\mathbf{Q}}{2}\downarrow}), \end{aligned} \quad (20)$$

while the continuum part results are very similar to Eq. (18),

$$\begin{aligned} S_{\text{cont}}^{zz}(\mathbf{k}, \omega) &= \frac{1}{4N} \sum'_{\mathbf{q}} (u_{\mathbf{q}} v_{\mathbf{k}+\mathbf{q}} - u_{\mathbf{k}+\mathbf{q}} v_{\mathbf{q}})^2 \\ &\quad \times \delta(\omega - (\omega_{\mathbf{q}\uparrow} + \omega_{\mathbf{k}-\mathbf{q}\downarrow})), \end{aligned} \quad (21)$$

except that in the sum over the triangular Brillouin zone the momentum \mathbf{q} satisfying $\mathbf{q} = \frac{\mathbf{Q}}{2}$ or $\mathbf{k} + \mathbf{q} = \frac{\mathbf{Q}}{2}$ are not taken into account. This is indicated by the primed sum.

From Eq. (20) it is clear that the spectral weight of the singular part is located at the shifted spinon excitations $\omega_{\mathbf{k}+\frac{\mathbf{Q}}{2}\uparrow}$ and $\omega_{\mathbf{k}-\frac{\mathbf{Q}}{2}\downarrow}$. However, we have recently shown [38] that—due to the coefficients in front of each δ function—the spectral

weight between both shifted spinon dispersions is redistributed in such a way that if one reconstructs a new dispersion from those pieces of the spinon dispersions with dominant spectral weight, the main features of the *one magnon* dispersion computed with the series expansion are recovered [18] (see, for instance, in Fig. 1 the $J^z = 1$ case). Notice that for the anisotropic case $S_{\text{sing}}^{zz}(\mathbf{k}, \omega)$ does not contain elastic processes at $\mathbf{k} = \pm\mathbf{Q}$. This is in contrast to the isotropic case where the condensation of up/down flavors occurs at both momenta, $\frac{\mathbf{Q}}{2}$ and $-\frac{\mathbf{Q}}{2}$. On the other hand, we have shown [38] that the remaining weak signal dispersion is related to unphysical excitations coming from the relaxation of the local constraint. In fact, to recover the proper low temperature behavior of thermodynamic properties such unphysical excitations must be discarded [33]. So, this simple procedure can be conceived as an approximate manner of carrying on the projection of the spectrum into the physical Hilbert space which, even numerically [42], is very difficult to implement in a calculation. We have called this procedure of reconstructing the one magnon excitation and eliminating the remnant weak signal *reconstructed* mean field Schwinger boson theory [33].

In Fig. 1 is shown the dynamical structure factor (intensity curve) within the reconstructed SBMF theory for different anisotropy values J^z/J along with the relation dispersion predicted by series expansion (SE) and linear spin wave theory (LSWT). It is observed that the low energy sector of the spectra predicted by the reconstructed SBMF theory reproduces quite well, qualitatively and quantitatively, the one magnon dispersion predicted by series expansion for the anisotropy range $0.4 \lesssim J^z/J \leq 1$. This agreement between the SBMF theory and SE along with that obtained for the local magnetization (Table I) give a strong support to the Schwinger boson mean field theory developed in Sec. III for the XXZ model [43].

IV. APPLICATION TO $\text{Ba}_3\text{CoSb}_2\text{O}_9$

In this section we explore the possible relation between the present spectrum of the XXZ model and that found in the INS experiments of $\text{Ba}_3\text{CoSb}_2\text{O}_9$. One important difference is that within the reconstructed SBMF the dominant spectral weight is mostly located at the low energy sector of the spectrum. However, given the proximity to a spin liquid phase proposed in the literature [12], it is important to investigate the spectrum once the ground state of the XXZ model is pushed near a spin liquid phase. In our approximation this situation can be induced by introducing exchange interactions to second neighbors. In fact, in the isotropic case, it is known [44,45] that there is a spin liquid phase for moderate J_2 values, $0.1 \leq J_2/J \leq 0.14$. Around these J_2 values, and for small anisotropy $J^z/J_2 = J^z/J = 0.8$, we have checked that the local magnetization is still quite robust but it is proximate to a spin liquid phase since it vanishes abruptly at $J_2/J \sim 0.25$. In Fig. 2 is shown the dynamical structure factor (intensity curve) for several values of J_2 . As J_2 increases there is an important spectral weight transfer from the low to the high energy sector of the spectrum. In particular, around $J_2/J = 0.15$ the extended continuum of two spinon excitations is recovered.

As at the mean field level the spectrum corresponds to two free spinon excitations, it is important to get some insight about the spinon spinon interaction once corrections to the mean field theory are included. Effective gauge field theory [4,24] predicts that for a commensurate spinon condensed phase there is a confinement of spinons, giving rise to spin-1 magnon excitations of the 120° Néel order. Within the context of the Schwinger bosons one should include Gaussian fluctuations [46] of the mean field parameters which is beyond the scope of the present work. Instead, we adopt a simpler strategy [33] that allows us to get a physical insight about the spinon spinon interactions once J_2 is included.

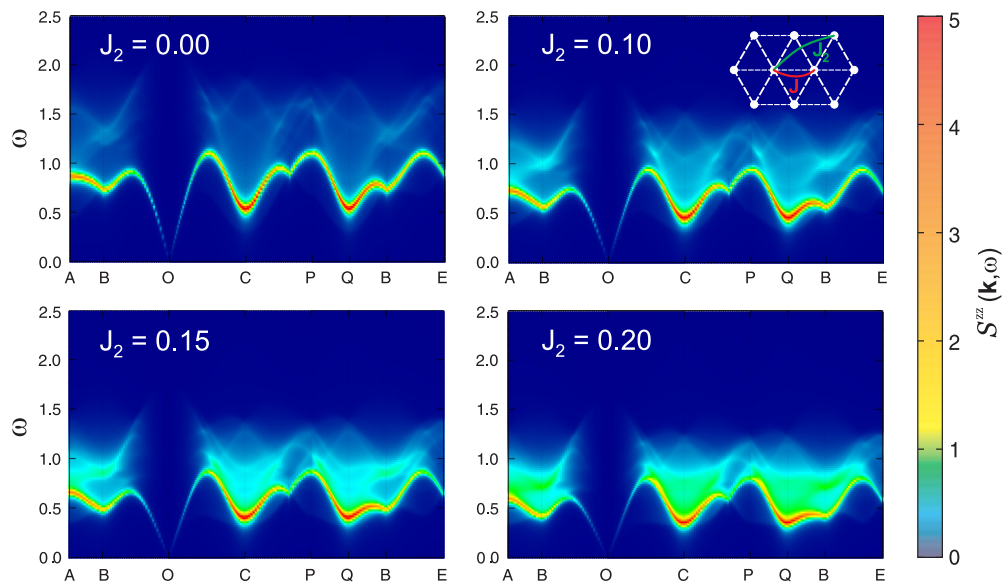


FIG. 2. (Color online) Dynamical structure factor predicted by the reconstructed SBMF theory (intensity curves) along the same path of the Brillouin zone of Fig. 1 for several second neighbors exchange values. The same anisotropy interaction $J^z/J = 0.8$, between first and second neighbors, has been selected. Inset: schematic representation of the exchange interactions on the triangular lattice. The values of J_2 are in units of J .

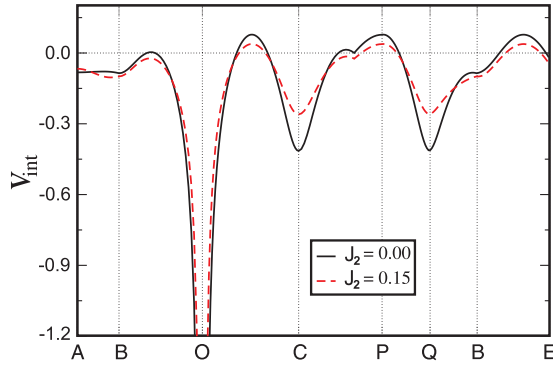


FIG. 3. (Color online) Spinon spinon interaction V_{int} predicted by the SBMF within the first order perturbation theory [Eq. (22)] for different J_2 values and $J^z/J = 0.8$. The values of J_2 are in units of J .

If the XXZ Hamiltonian is split as $H = H_{\text{MF}} + V$, the interaction term is given by $V = H - H_{\text{MF}}$. Then, the effect of V on a two free spinon state $|2s\rangle = |\mathbf{q}\uparrow; \mathbf{p}\downarrow\rangle = \alpha_{\mathbf{q}\uparrow}^\dagger \alpha_{\mathbf{p}\downarrow}^\dagger |gs\rangle$ is computed, to first order in perturbation theory, as the energy of creating two spinons above the ground state as $E_{2s} = \langle 2s|H|2s\rangle - \langle gs|H|gs\rangle$. Therefore, the interaction between the two spinons results in $V_{\text{int}} = \bar{E}_{2s} - E_{2s}^{\text{MF}}$, where $E_{2s}^{\text{MF}} = \langle 2s|H_{\text{MF}}|2s\rangle - \langle gs|H_{\text{MF}}|gs\rangle = \omega_{\mathbf{q}\uparrow} + \omega_{\mathbf{p}\downarrow}$ [47]. The spinon interaction thus calculated turns out to be

$$V_{\text{int}} = \frac{1}{N} \left[\gamma_{\mathbf{q}+\mathbf{p}} (u_{\mathbf{q}} v_{\mathbf{p}} + v_{\mathbf{q}} u_{\mathbf{p}})^2 + \frac{J^z}{J} \gamma_{\mathbf{q}-\mathbf{p}} (v_{\mathbf{q}} v_{\mathbf{p}} - u_{\mathbf{q}} u_{\mathbf{p}})^2 + \frac{J^z}{J} 3(J + J_2) \right], \quad (22)$$

where $\gamma_{\mathbf{k}-\mathbf{p}} = \frac{1}{4} \sum_{\delta} J_{\delta} e^{i(\mathbf{k}-\mathbf{p})\cdot\delta}$. In Fig. 3 is plotted the spinon spinon interaction V_{int} for a pair of spinons $|\frac{\mathbf{Q}}{2}\uparrow; \mathbf{k} - \frac{\mathbf{Q}}{2}\downarrow\rangle$ building up the lowest magnon excitation of momentum \mathbf{k} , for $J^z/J = 0.8$, $J_2 = 0$ (solid line), and $J_2 = 0.2$ (dashed line). It is observed that the attraction between two spinons building up the magnon excitation at $\mathbf{k} = 0$ is very strong, while for $\mathbf{k} = \pm\mathbf{Q}$ the attraction is still, relatively, important. On the other hand, for momenta outside the neighborhood of $\mathbf{k} = 0$ and $\mathbf{k} = \pm\mathbf{Q}$ the attraction of spinon excitations is much weaker. These results agree with the physical picture of tightly bound and weakly bound spinons building up the lower and higher energy magnon excitations, respectively, although within the context of the first order perturbation theory, it is not completely justified. Interestingly, as J_2 is introduced there is, in general, a weakening of the spinon spinon interaction for almost all momenta (dashed line of Fig. 3). These results give us a deeper insight of the mean field spectrum. For instance, the spectral weight concentrated at low energy around points C and Q (see $J_2 = 0$ case of Fig. 2) can be correlated to the presence of tightly bound pairs of spinons building up the magnon excitation, whereas as soon as J_2 is increased the spectral weight transfer from low to high energies, along with the appearance of the extended continuum, can be consistently interpreted as the proliferation of nearly free pairs of spinons above the one magnon excitations.

In order to make a closer comparison with the INS experiments performed in $\text{Ba}_3\text{CoSb}_2\text{O}_9$, in the bottom panel

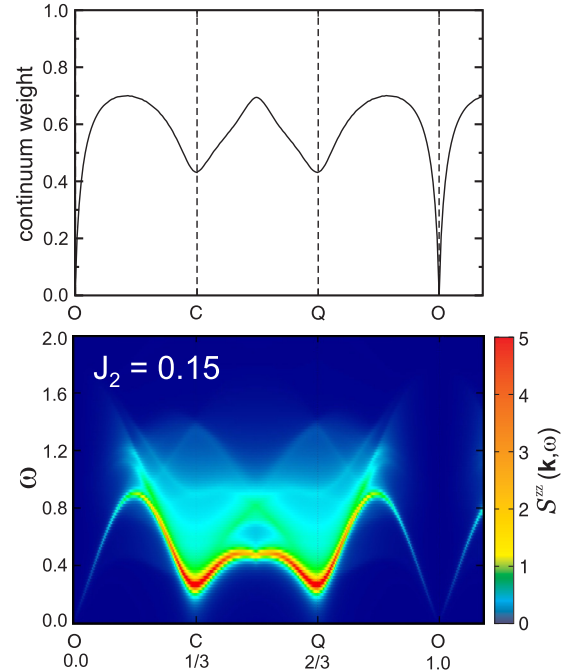


FIG. 4. (Color online) Bottom panel: dynamical structure factor predicted by the reconstructed SBMF theory (intensity curves) along the experimental path [see Fig. 4(d) of Ref. [12]] for $J^z/J = 0.9$. In the horizontal axis the cut along $[\text{H H } 0]$ direction is depicted, in units of 4π , as in Ref. [12]. Top panel: relative weight of the two spinon continuum $\int S_{\text{cont}}^{zz}(\mathbf{k}, \omega) d\omega / S^{zz}(\mathbf{k})$. The value of J_2 is in units of J .

of Fig. 4 is shown the spectrum predicted by the SBMF theory for $J_2/J = 0.15$ and $J^z/J = 0.9$ along the experimental path. If one compares with Fig. 4(d) of Ref. [12] there is qualitatively good agreement although the dominant high energy spectral weight with respect to the magnon excitation is not completely recovered by the SBMF theory. However, if one separates the spectral weight $S_{\text{sing}}^{zz}(\mathbf{k}, \omega)$ of the low energy magnon excitations from the high energy continuum it is possible to quantify the relative weight of the two spinon continuum in the spectrum by computing $\int S_{\text{cont}}^{zz}(\mathbf{k}, \omega) d\omega / S^{zz}(\mathbf{k})$, where $S^{zz}(\mathbf{k}) = \int S^{zz}(\mathbf{k}, \omega) d\omega$. The top panel of Fig. 4 shows an important amount and \mathbf{k} dependence of the continuum contribution for $J_2 = 0.15$.

V. CONCLUSIONS

In conclusion, we have performed a series expansion and a mean field Schwinger boson study of the antiferromagnetic XXZ model on the triangular lattice. The series expansion results reveal a rotonlike excitation minima at the middle points of the edges of the Brillouin zone for all range of anisotropy $0 \leq J^z/J \leq 1$. On the other hand, we have extended the Schwinger boson theory to four bond operators and fully computed static and dynamic properties at the mean field level. The good agreement between the mean field Schwinger boson and the series expansion for the spin wave dispersion relation encouraged us to extend the microscopic model by including exchange interaction to second neighbors in order to qualitatively reproduce the unusual spectrum of the $\text{Ba}_3\text{CoSb}_2\text{O}_9$ compound. By correlating the main features of the mean field

spectrum with the spinon spinon interaction we provide a coherent theoretical calculation supporting the idea [12] that the extended continuum observed in the INS experiments in $\text{Ba}_3\text{CoSb}_2\text{O}_9$ can be interpreted as the fractionalization of magnon excitations in 2D. Of course, it would be interesting to test the presence of exchange interaction to second neighbors in this compound. Another important issue would be to classify the possible spin liquid phases of the XXZ model within a projective symmetry group analysis [2,48,49]. Interestingly, using the Schwinger fermions [50] in the square lattice it has been recently found that the variety of spin liquid phases for a

Hamiltonian with $U(1) \times Z_2$ symmetry is even richer than the $SU(2)$ symmetry case.

ACKNOWLEDGMENTS

We thank C. Batista for the exchange of useful information regarding the $\text{Ba}_3\text{CoSb}_2\text{O}_9$ compound. This work was in part supported by CONICET (PIP2012) under Grant No. 1060, by the US National Science Foundation Grant No. DMR-1306048, and by the computing resources provided by the Australian (APAC) National facility.

-
- [1] P. W. Anderson, *Mater. Res. Bull.* **8**, 153 (1973); P. Fazekas and P. W. Anderson, *Philos. Mag.* **30**, 423 (1974).
- [2] X. G. Wen, *Phys. Rev. B* **65**, 165113 (2002).
- [3] See, for example, G. Misguich and C. Lhuillier, *Frustrated Spin Systems*, edited by H. T. Diep (World Scientific, Singapore, 2004), [arXiv:cond-mat/0310405](https://arxiv.org/abs/cond-mat/0310405) and reference therein.
- [4] S. Sachdev, *Nat. Phys.* **4**, 173 (2008).
- [5] L. Balents, *Nature (London)* **464**, 199 (2010).
- [6] T. Senthil, A. Vishwanath, L. Balents, S. Sachdev, and M. P. A. Fisher, *Science* **303**, 1490 (2004).
- [7] B. J. Powell and R. H. McKenzie, *Rep. Prog. Phys.* **74**, 056501 (2011).
- [8] L. D. Faddeev and L. A. Takhtajan, *Phys. Lett. A* **85**, 375 (1981).
- [9] S. E. Nagler, D. A. Tennant, R. A. Cowley, T. G. Perring, and S. K. Satija, *Phys. Rev. B* **44**, 12361 (1991); D. A. Tennant, T. G. Perring, R. A. Cowley, and S. E. Nagler, *Phys. Rev. Lett.* **70**, 4003 (1993); M. Mourigal, M. Enderle, A. Klöpperpieper, J. S. Caux, A. Stunault, and H. M. Ronnow, *Nat. Phys.* **9**, 435 (2013).
- [10] R. Coldea, D. A. Tennant, A. M. Tsvetlik, and Z. Tylczynski, *Phys. Rev. Lett.* **86**, 1335 (2001).
- [11] T. H. Han, J. S. Helton, S. Chu, D. G. Nocera, J. A. Rodriguez-Rivera, C. Broholm, and Y. S. Lee, *Nature (London)* **492**, 406 (2012).
- [12] H. D. Zhou, C. Xu, A. M. Hallas, H. J. Silverstein, C. R. Wiebe, I. Umegaki, J. Q. Yan, T. P. Murphy, J. H. Park, Y. Qiu, J. R. D. Copley, J. S. Gardner, and Y. Takano, *Phys. Rev. Lett.* **109**, 267206 (2012).
- [13] Y. Shirata, H. Tanaka, A. Matsuo, and K. Kindo, *Phys. Rev. Lett.* **108**, 057205 (2012).
- [14] T. Susuki, N. Kurita, T. Tanaka, H. Nojiri, A. Matsuo, K. Kindo, and H. Tanaka, *Phys. Rev. Lett.* **110**, 267201 (2013).
- [15] G. Koutroulakis, T. Zhou, Y. Kamiya, J. D. Thompson, H. D. Zhou, C. D. Batista, and S. E. Brown, *Phys. Rev. B* **91**, 024410 (2015).
- [16] M. Kohno, O. A. Starykh, and L. Balents, *Nat. Phys.* **3**, 790 (2007).
- [17] D. Heidarian, S. Sorella, and F. Becca, *Phys. Rev. B* **80**, 012404 (2009).
- [18] W. Zheng, J. O. Fjaerestad, R. R. P. Singh, R. H. McKenzie, and R. Coldea, *Phys. Rev. Lett.* **96**, 057201 (2006).
- [19] M. Mourigal, W. T. Fuhrman, A. L. Chernyshev, and M. E. Zhitomirsky, *Phys. Rev. B* **88**, 094407 (2013).
- [20] D. P. Arovas and A. Auerbach, *Phys. Rev. B* **38**, 316 (1988); A. Auerbach and D. P. Arovas, *Phys. Rev. Lett.* **61**, 617 (1988).
- [21] J. E. Hirsch and S. Tang, *Phys. Rev. B* **39**, 2850 (1989); S. Sarker, C. Jayaprakash, H. R. Krishnamurthy, and M. Ma, *ibid.* **40**, 5028 (1989).
- [22] P. Chandra, P. Coleman, and A. I. Larkin, *J. Phys.: Condens. Matter* **2**, 7933 (1990).
- [23] H. A. Ceccatto, C. J. Gazza, and A. E. Trumper, *Phys. Rev. B* **47**, 12329 (1993).
- [24] N. Read and S. Sachdev, *Phys. Rev. Lett.* **66**, 1773 (1991); S. Sachdev and N. Read, *Int. J. Mod. Phys. B* **5**, 219 (1991).
- [25] A. A. Burkov and A. H. MacDonald, *Phys. Rev. B* **66**, 115320 (2002).
- [26] W. Zheng, J. O. Fjaerestad, R. R. P. Singh, R. H. McKenzie, and R. Coldea, *Phys. Rev. B* **74**, 224420 (2006).
- [27] J. Oitmaa, C. Hamer, and W. Zheng, *Series Expansion Methods for Strongly Interacting Lattice Models* (Cambridge University Press, Cambridge, UK, 2006).
- [28] M. P. Gelfand and R. R. P. Singh, *Adv. Phys.* **49**, 93 (2000).
- [29] A. L. Chernyshev and M. E. Zhitomirsky, *Phys. Rev. B* **79**, 144416 (2009).
- [30] J. Alicea, O. I. Motrunich, and M. P. A. Fisher, *Phys. Rev. B* **73**, 174430 (2006).
- [31] O. A. Starykh, A. V. Chubukov, and A. G. Abanov, *Phys. Rev. B* **74**, 180403(R) (2006).
- [32] N. Elstner, R. R. P. Singh, and A. P. Young, *Phys. Rev. Lett.* **71**, 1629 (1993).
- [33] A. Mezio, L. O. Manuel, R. R. P. Singh, and A. E. Trumper, *New J. Phys.* **14**, 123033 (2012).
- [34] C. J. De Leone and G. T. Zimanyi, *Phys. Rev. B* **49**, 1131 (1994).
- [35] Y. Fukumoto, *J. Phys. Soc. Jpn.* **65**, 569 (1996).
- [36] Under time reversal the spinor transforms as $(b_{i\uparrow}, b_{i\downarrow}) \rightarrow (b_{i\downarrow}, -b_{i\uparrow})$.
- [37] In this case it is expected that the mean field parameters behave as $\langle \hat{A}_{ij} \rangle = \iota S \sin \frac{Q}{2} \cdot (\mathbf{r}_j - \mathbf{r}_i)$, $\langle \hat{B}_{ij} \rangle = S \cos \frac{Q}{2} \cdot (\mathbf{r}_j - \mathbf{r}_i)$, $\langle \hat{C}_{ij} \rangle = \iota S \cos \frac{Q}{2} \cdot (\mathbf{r}_j - \mathbf{r}_i)$, and $\langle \hat{D}_{ij} \rangle = S \sin \frac{Q}{2} \cdot (\mathbf{r}_j - \mathbf{r}_i)$.
- [38] A. Mezio, C. N. Sposetti, L. O. Manuel, and A. E. Trumper, *Eur. Phys. Lett.* **94**, 47001 (2011).
- [39] A. Mezio, C. N. Sposetti, L. O. Manuel, and A. E. Trumper, *J. Phys.: Condens. Matter* **25**, 465602 (2013).
- [40] K. Lefmann and P. Hedegård, *Phys. Rev. B* **50**, 1074 (1994).
- [41] F. Mila, *Phys. Rev. B* **42**, 2677 (1990).
- [42] T. Li, F. Becca, W. Hu, and S. Sorella, *Phys. Rev. B* **86**, 075111 (2012).

- [43] Using the identities; $\hat{C}_{ij}^\dagger \hat{C}_{ij} + \hat{D}_{ij}^\dagger \hat{D}_{ij} = S^2$ and $\hat{B}_{ij}^\dagger \hat{B}_{ij} + \hat{A}_{ij}^\dagger \hat{A}_{ij} = S^2$ for $i \neq j$, the XXZ model can be written in terms of two, three, or four bond operator, with the latter being the most appropriate one.
- [44] R. Kaneko, S. Morita, and M. Imada, *J. Phys. Soc. Jpn.* **83**, 093707 (2014).
- [45] L. O. Manuel and H. A. Ceccatto, *Phys. Rev. B* **60**, 9489 (1999).
- [46] A. E. Trumper, L. O. Manuel, C. J. Gazza, and H. A. Ceccatto, *Phys. Rev. Lett.* **78**, 2216 (1997).
- [47] Here the xy part of E_{2s} is rescaled as $\overline{E}_{2s}^{xy} = \frac{1}{2} E_{2s}^{xy}$ in order to compensate the difference, $\langle \text{gs} | H^{xy} | \text{gs} \rangle = 2 \langle \text{gs} | H_{\text{MF}}^{xy} | \text{gs} \rangle$, between the application of Wick's theorem and mean field decoupling.
- [48] F. Wang and A. Vishwanath, *Phys. Rev. B* **74**, 174423 (2006).
- [49] L. Messio, C. Lhuillier, and G. Misguich, *Phys. Rev. B* **87**, 125127 (2013).
- [50] J. Reuther, S.-P. Lee, and J. Alicea, *Phys. Rev. B* **90**, 174417 (2014).